JOURNAL OF VIROLOGY, Sept. 2002, p. 8797–8807 Vol. 76, No. 17
0022-538X/02/$04.00+0 DOI: 10.1128/JVI.76.17.8797–8807.2002

Viral Interferon Regulatory Factor 1 of Kaposi's Sarcoma-Associated Herpesvirus Interacts with a Cell Death Regulator, GRIM19, and Inhibits Interferon/Retinoic Acid-Induced Cell Death

Taegun Seo,[1] Daeyoup Lee,[1] Young Sam Shim,[1] Jon E. Angell,[2] Natesa V. Chidambaram,[2] Dhananjaya V. Kalvakolanu,[2] and Joonho Choe[1]*

Department of Biological Sciences, Korea Advanced Institute of Science and Technology, Daejeon 305-701, Korea,[1] and Department of Microbiology and Immunology, Greenebaum Cancer Center, Molecular and Cellular Biology Program, University of Maryland School of Medicine, Baltimore, Maryland 21201[2]

Received 7 February 2002/Accepted 4 June 2002

Kaposi's sarcoma-associated herpesvirus (KSHV) plays a significant role in the development of Kaposi's sarcoma, primary effusion lymphoma, and some forms of multicentric Castleman's disease. The KSHV open reading frame K9 encodes the viral interferon (IFN) factor 1 (vIRF1), which downregulates IFN- and IRF-mediated transcriptional activation, and leads to cellular transformation in rodent fibroblasts and induction of tumors in nude mice. Using the yeast two-hybrid assay, we identified genes associated with retinoid-IFN-induced mortality-19 (GRIM19), which interacts directly with vIRF1, both in vivo and in vitro. The N-terminal region of vIRF1 is required for binding GRIM19. Colocalization of vIRF1 and GRIM19 was observed in 293T cells. The vIRF1 protein deregulates GRIM19-induced apoptosis in the presence of IFN/all-trans-retinoic acid (RA) and inhibits IFN/RA-induced cell death. Another DNA tumor viral protein, human papillomavirus type 16 E6, also binds GRIM19, suggesting that this is a general target of viral proteins. Our results collectively indicate that vIRF1 modulates IFN/RA-cell death signals via interactions with GRIM19.

Kaposi's sarcoma (KS)-associated herpesvirus (KSHV), also called human herpesvirus 8 (HHV8), is a recently discovered human DNA tumor virus that plays a critical role in the development of KS lesions, body cavity-based primary effusion lymphoma, and a subset of multicentric Castleman's disease (5, 6, 43). KSHV belongs to the gammaherpesvirus group and displays significant genetic similarity to herpesvirus saimiri and Epstein-Barr virus (39). Viral infection triggers the activity of multiple interferons (IFNs), which participate in host immune surveillance. IFNs exhibit a wide range of biological activities, including cell growth inhibition and immune activation. Viruses have developed a variety of strategies to cope with the inhibitory effects of IFNs (35). IFN regulatory factors (IRFs) are transcription factors that serve as mediators of the IFN signal. Interestingly, KSHV contains at least three open reading frames (ORFs) encoding proteins homologous to IRF families, designated viral IRFs (vIRFs). These include ORF K9 (also known as vIRF1), vIRF2, and vIRF3 or latent-associated nuclear antigen 2 (3, 24, 29, 37).

The vIRF1 protein comprises 449 amino acids (aa) with an N-terminal region containing a conserved tryptophan-rich DNA-binding region and displaying 70% identity to the IFN consensus sequence binding protein (39). In a transient-transfection assay, vIRF1 represses IFN- and IRF1-mediated transcription (24, 48). NIH 3T3 cells that stably express vIRF1 undergo transformation and consequently display features of malignant fibrosarcoma in nude mice (14, 24). Recently, we and another group reported that vIRF1 associates with the tumor suppressor p53 protein, leading to the repression of p53-dependent transcription and apoptosis (33, 41). These observations collectively indicate that vIRF1 induces tumorigenicity. The vIRF1 protein associates with p300/CREB binding protein (CBP), leading to the inhibition of transactivation of CBP, histone acetyltransferase activity of p300 and the formation of transcriptionally active IRF3-p300/CBP complexes (4, 23, 25, 40). Earlier studies have demonstrated that vIRF1 acts as a transcriptional activator, despite its many repressive activities (38).

The importance of the IFN pathway in cell growth suppression is confirmed in a number of reports (17, 20, 44). In addition to IFNs, all-trans retinoic acid (RA) and its derivatives are important in tumor suppression (27, 45). Clinical studies show that a combination of IFN and RA inhibits cell growth in vitro and in vivo more potently than either agent alone (26, 28, 31). Hofmann et al. (18) identified the specific genes that play a role in IFN/RA-induced cell death by an antisense technical-knockout approach (8). These genes were designated according to their association with retinoid-IFN-induced mortality (i.e., GRIMs). Out of these, GRIM12 is identical to human thioredoxin reductase. Overexpression of GRIM12 causes a small amount of cell death and increases the susceptibility of cells to IFN/RA-induced cell death. GRIM12 modulates the activity of capase-8 and increases the expression of death receptors to evoke cell death (18, 30). Another GRIM gene, GRIM19, was also characterized (1). GRIM19 is a novel cell death-associated gene that is not included in any of the known death gene categories. This gene encodes a 144-aa protein that localizes predominantly to the nucleus. A sequence search revealed that other species, specifically, mice, *Arabidopsis thaliana*, and *Staphylococcus aureus*, as well as humans, contain the

* Corresponding author. Mailing address: Department of Biological Sciences, Korea Advanced Institute of Science and Technology, Daejeon 305-701, Korea. Phone: 82-42-869-2630. Fax: 82-42-869-5630. E-mail: jchoe@mail.kaist.ac.kr.

GRIM19 gene, suggesting that the protein is ubiquitous in most organisms. Overexpression of GRIM19 enhances caspase-9 activity and apoptotic cell death in response to IFN/RA treatment (1). GRIM19 is located in the 19p13.2 region of the human chromosome essential for prostate tumor suppression, signifying that the protein may be a novel tumor suppressor (7).

To transform cells and induce tumors, various tumor suppressors need to be inactivated, which may occur in a number of ways. Since vIRF1 triggers cellular transformation without the aid of any other oncogenic protein, we reasoned that, in addition to p53 and p300/CBP, the viral protein may target factors participating in other cell death pathways. Using the yeast two-hybrid assay with vIRF1 as bait, we identified the newly characterized cell death regulatory protein, GRIM19, as a novel interaction partner. This interaction specifically suppresses the cell death activity of GRIM19 in response to IFN/RA.

MATERIALS AND METHODS

Plasmids. The pcDNA3-vIRF1 construct was described previously (40). To generate glutathione *S*-transferase (GST)-tagged vIRF1 and its deletion mutants, the corresponding cDNA sequences from pcDNA3-vIRF1 were subcloned into pGEX4T-1 (Amersham Pharmacia Biotech, Uppsala, Sweden). The pGBKT7-vIRF1ΔC plasmid, which was used as bait for the yeast two-hybrid screen, was generated by cloning into the *Eco*RI/*Sal*I sites of pGBKT7. To obtain FLAG-tagged vIRF1 and its N-terminal deletion mutants, the corresponding cDNA sequences were cloned into the *Hin*dIII/*Bgl*II sites of pFIN, thus generating pFIN-vIRF1 and pFIN-vIRF1ΔN, respectively. GAL4 DNA-binding domain (DBD) fused to vIRF1 was constructed by inserting the *Eco*RI/*Not*I fragment from pcDNA3-vIRF1 into the corresponding restriction sites of pcDNA3-GAL4 (including the cytomegalovirus promoter) to generate a chimeric protein with GAL4 DBD fused to the N terminus of the viral factor. GRIM19 cDNA was amplified by PCR with pCXN2-GRIM19 plasmid as a template, as described previously (1). Amplified products were digested with appropriate restriction enzymes and cloned into the *Eco*RI/*Xho*I sites of pcDNA3, pcDNA3-HA, and pGADT7, respectively. The *Eco*RI/*Xho*I fragment of pcDNA3-GRIM19 was cloned into the *Eco*RI/*Sal*I sites of pGEX4T-1 and pVP16 (Clontech, Palo Alto, Calif.). To generate a GST-GRIM19 expression plasmid, the *Bam*HI/*Not*I fragment from pGEX4T-1–GRIM19 was inserted into the corresponding restriction sites of the pEBG vector (including the EF-1α promoter) to generate a chimeric protein with GST fused to the N terminus of GRIM19. The pEGFP-GRIM19 construct expressing green fluorescent protein (GFP) fused to vIRF1 was generated by subcloning into the *Bgl*II/*Sal*I sites of pEGFP-C1 (Clontech). pcDNA3-E1A and pcDNA3-E6 were generated by inserting the required sequences into the *Eco*RI/*Xho*I sites of pcDNA3. The pSG5-simian virus 40 (SV40) large T (LT) antigen was a generous gift from T. M. Roberts (Dana-Farber Cancer Institute). The pFR-Luc plasmid was described previously (22, 40).

Yeast two-hybrid assay. Yeast two-hybrid screening was performed by using the Matchmaker GAL4 Two-Hybrid System 3 (Clontech). The yeast strain, AH109 (19), containing pGBKT7-vIRF1ΔC was transformed with a human brain cDNA library cloned into a GAL4 activation domain vector, pACT2 (Clontech). Transformants were selected on plates containing synthetic dextrose (SD)–glucose–20 mM 3-amino-1,2,4-triazole (3-AT) lacking tryptophan (−Trp), leucine (−Leu), and histidine (−His) or on plates containing SD-glucose but lacking tryptophan, leucine, histidine, and adenine (−Ade). Library plasmids of positive clones were isolated, subcloned into the pcDNA3 vector, and sequenced with a T7 promoter primer.

Cell culture and transfection. 293T and HeLa cells were grown in Dulbecco modified Eagle medium supplemented with 10% fetal bovine serum. BJAB, BCBL-1, and MCF-7 cells were maintained in RPMI 1640 containing 10% fetal bovine serum. Transfections were performed by the calcium phosphate method (16) in 293T cells. HeLa cells were transfected with Superfect transfection reagent (Qiagen, Hilden, Germany) according to the manufacturer's recommendations. To generate stable cells expressing FLAG-vIRF1 and FLAG-vIRF1ΔN, MCF-7 cells were transfected with pFIN-vIRF1 and pFIN-vIRF1ΔC by using Lipofectamine Plus reagent (Gibco-BRL, Gaithersburg, Md.) according to the manufacturer's instructions. Transfected cells were selected for 3 weeks in complete medium supplemented with 1 mg of G418 (Gibco-BRL)/ml.

Coimmunoprecipitation. 293T cells were transiently transfected either with GST or GST-GRIM19 in combination with FLAG-vIRF1, or with control plasmid (pFIN), FLAG-vIRF1, in conjunction with hemagglutinin (HA)-GRIM19. After 48 h of transfection, cells were lysed in EBC buffer (50 mM Tris-HCl, pH 7.5; 120 mM NaCl; 0.5% Nonidet P-40; 50 mM NaF; 200 μM sodium orthovanadate; 1 mM phenylmethylsulfonyl fluoride) and incubated with glutathione-Sepharose 4B beads or protein G-Sepharose beads (preincubated with anti-FLAG monoclonal antibody [Sigma, St. Louis, Mo.]) at 4°C for 2 h with rocking. Bound protein complexes were washed three times with EBC buffer and then resuspended in loading buffer (10 μl). Samples were immunoblotted with anti-FLAG, anti-GST, or anti-HA antibody, respectively. BJAB and TPA (12-*O*-tetradecanoylphorbol-13-acetate)-treated BCBL-1 cells were lysed with EBC buffer and immunoprecipitated with anti-GRIM19 mouse monoclonal antibody, as described above. Samples were immunoblotted with anti-vIRF1 rabbit polyclonal antibody.

GST pull-down assay. Wild-type GST and GST fusion proteins were prepared by induction of *Escherichia coli* containing the fusion vector with 1 mM IPTG (isopropyl-β-D-thiogalactopyranoside). After lysis by sonication, GST fusion proteins were bound to glutathione-Sepharose 4B beads, washed with phosphate-buffered saline (PBS), and eluted with buffer containing 25 mM glutathione. ^{35}S-labeled proteins were synthesized in vitro by using the TNT-Coupled Transcription-Translation System (Promega, Madison, Wis.) as described by the manufacturer. Purified or Sepharose 4B-bound GST fusion protein was incubated with ^{35}S-labeled proteins in 500 μl of binding buffer (50 mM Tris-HCl, pH 7.5; 150 mM NaCl; 5 mM EDTA, pH 8.0; 2.5 mM dithiothreitol; 0.7 mg of bovine serum albumin [BSA]/ml; 0.1% Nonidet P-40) at 4°C for 90 min. The precipitated protein complexes were washed five times with binding buffer. Bound proteins were analyzed by sodium dodecyl sulfate-polyacrylamide gel electrophoresis (SDS-PAGE) and autoradiography.

Immunofluorescence. Cells were fixed with 3.7% formaldehyde for 30 min, permeabilized with PBS containing 0.2% Triton X-100 (PBST) on ice, blocked with 1% BSA, incubated with primary antibody in PBST containing 1% BSA for 1 h at room temperature, and washed three times with PBST. Cells were incubated with secondary antibody in PBST containing 1% BSA for 1 h and washed three times with PBST. Analyses were performed with a Zeiss (Oberkochen, Germany) confocal microscope with fluorescein isothiocyanate (FITC) and TRITC (tetramethyl rhodamine isothiocyanate) filter sets. The Nucleus of cell was stained with DAPI (4′,6′-diamidino-2-phenylindole; Sigma, St. Louis, Mo.).

Apoptosis assay. HeLa cells grown on coverslips in 35-mm-diameter dishes were transfected with Superfect reagent. Cells were treated with IFN-β (3,000 U/ml; Calbiochem, San Diego, Calif.), together with RA (5 μM; Sigma), for 72 h and fixed. The TUNEL (terminal deoxynucleotidyltransferase-mediated dUTP-biotin nick end labeling) reaction (15) was performed with an in situ cell detection kit, as specified by the manufacturer (Roche Molecular Biochemicals, Mannheim, Germany). Analyses were performed with a Zeiss confocal microscope by using an FITC filter set. The percentage of apoptosis was determined by counting the green apoptotic cells from multiple fields.

Cell growth assay. Cell growth was measured with the Sulforhodamine-B (SRB) method (42) at 3, 5, and 7 days after IFN/RA treatment, respectively. Each group comprised eight replicates. Cells (3,000 cells/well) were plated in 96-well plates 6 h before IFN/RA treatment. Next, cells were fixed with 10% trichloroacetic acid at 4°C for 1 h, washed in water four times, stained with 0.4% SRB (dissolved in 1% acetic acid), and rinsed four times with 1% acetic acid. Bound dye was eluted with 100 μl of 10 mM Tris-HCl (pH 10.5), and each absorbance value was measured at 570 nm. One plate was fixed at 6 h after the cells were plated, and the absorbance value obtained was taken as 0% growth. The absorbance values obtained from untreated cells were taken as 100% growth. The changes in absorbance values in experimental wells relative to the initial value were measured as cell growth and death, respectively. When plotted as a percentage of untreated control growth and death, values measured were on the positive and negative scales of the *y* axis, respectively.

RESULTS

Identification of cellular proteins interacting with vIRF1. A yeast two-hybrid assay was performed to identify cellular proteins that interact with vIRF1. Since vIRF1 is a strong transactivator (38, 40), the C-terminal deletion construct, vIRF1ΔC (aa 1 to 360) fused to the DBD of GAL4, was used as bait (Fig.

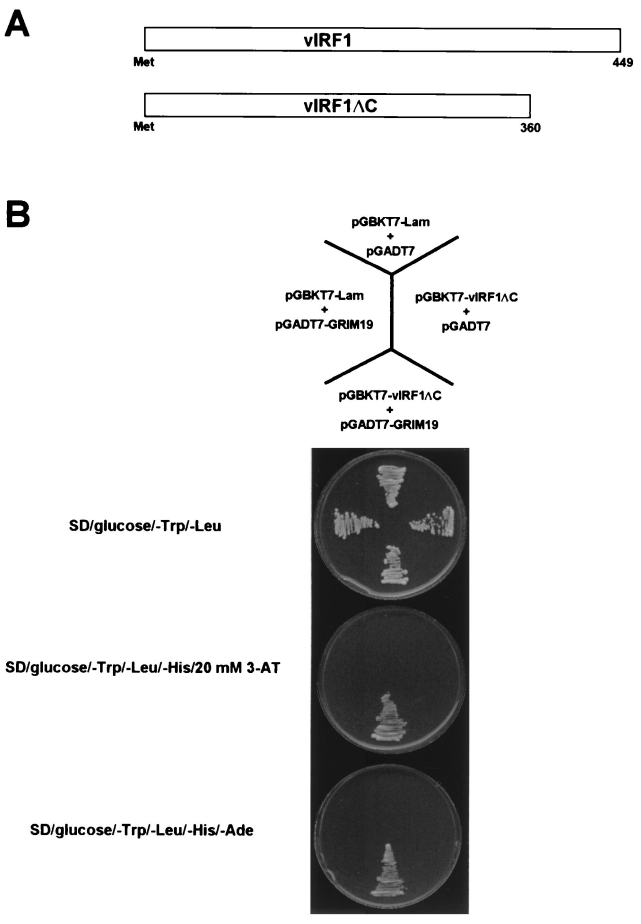

FIG. 1. Identification of GRIM19 as a vIRF1-interacting protein. (A) Schematic representation of vIRF1 used in yeast two-hybrid assay. The top diagram shows wild-type vIRF1; the diagram below displays vIRF1ΔC, a C-terminal deletion mutant of vIRF1. vIRF1ΔC was used as bait in the yeast two-hybrid assay. (B) A yeast strain, AH109, was transformed with various combinations of plasmids pGBKT7-Lamin C, pGBKT7-vIRF1ΔC, pGADT7, and pGADT7-GRIM19. Transformants were selected on SD–glucose–(−Trp, −Leu) plates. Yeast cells were streaked on SD–glucose–(−Trp, −Leu), SD–glucose–(−Trp, −Leu, −His)–20 mM 3-AT, and SD–glucose–(−Trp, −Leu, −His, −Ade) plates.

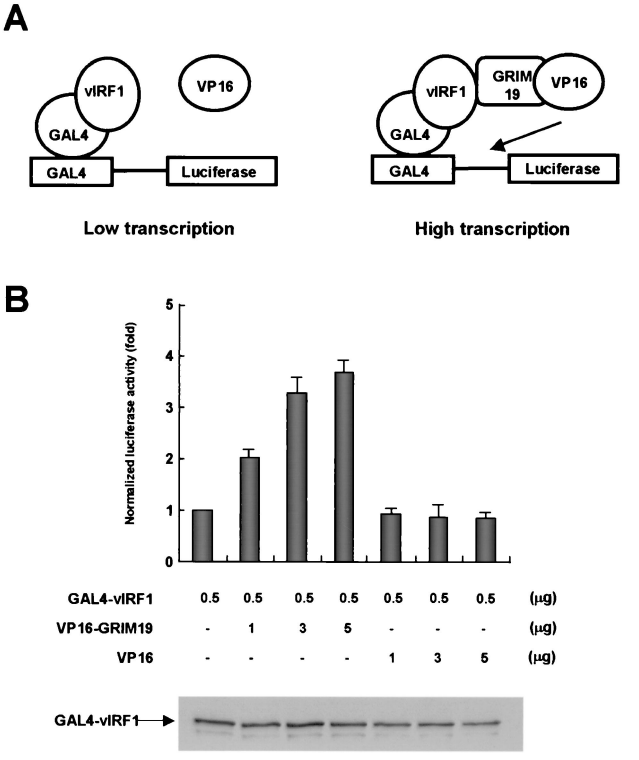

FIG. 2. Mammalian two-hybrid assay for the detection of vIRF1-GRIM19 interactions. (A) Schematic representation of a mammalian two-hybrid assay. (B) Mammalian two-hybrid assay of vIRF1 and GRIM19. vIRF1 fused to the GAL4 DBD interacted with GRIM19 fused to the VP16 activation domain. 293T cells were cotransfected with a GAL4-Luc reporter plasmid (pFR-Luc) (1 μg), Rous sarcoma β-galactosidase expression plasmid (pRSV-β-gal; 0.5 μg), expression plasmid of GAL4 DBD fused to vIRF1 (pcDNA-GAL4-vIRF1; 0.5 μg), and increasing amounts of either the expression plasmid encoding VP16 activation domain fused to GRIM19 (pVP16-GRIM19) or the plasmid encoding VP16 activation domain (pVP16). Transcriptional changes were measured by using the luciferase activity and presented as the fold activation. The luciferase activity was derived from three independent experiments and normalized with β-galactosidase expression levels. Equal amounts of total cellular extracts were resolved by SDS-PAGE and immunoblotted with anti-GAL4 DBD monoclonal antibody (Santa Cruz Biotechnology, Santa Cruz, Calif.).

1A). GAL4-fused vIRF1ΔC did not activate reporter gene expression independently in yeast (Fig. 1B). We screened a human brain cDNA library expressing proteins fused to the GAL4 transcriptional activation domain. From 10^6 yeast transformants we isolated 38 clones that activated a reporter gene in the presence of GAL4-fused vIRF1ΔC. Among these, three were identified as GRIM19, a novel cell death-related gene (1). The remaining 35 clones encode eight novel and two known proteins. To confirm interactions between vIRF1 and GRIM19, we cotransformed pGBKT7-Lamin C, pGBKT7-vIRF1ΔC, pGADT7, and pGBKT7-GRIM19 into the AH109 strain. Since human lamin C neither forms complexes nor interacts with most other unrelated proteins, this was used as a negative control (47). Only yeast cells containing pGBKT7-vIRF1ΔC and pGADT7-GRIM19 were grown on SD–glucose–(−Trp, −Leu, −His)–20 mM 3-AT and SD–glucose–(−Trp, −Leu, −His, −Ade) plates, respectively, indicating that vIRF1 specifically interacts with GRIM19 (Fig. 1B). To suppress leaky expression of HIS3, SD–glucose–(−Trp, −Leu, −His) plates were supplemented with 3-AT, a competitive inhibitor of the yeast HIS3 protein (9).

vIRF1 interacts with GRIM19. To verify the specific interactions between vIRF1 and GRIM19, a mammalian two-hybrid assay was performed (22). Two chimeric proteins were created by fusing full-length vIRF1 to DBD of GAL4 (GAL4-vIRF1) and full-length GRIM19 to the transcriptional activation domain of VP16 (VP16-GRIM19). Transient-cotransfection experiments were performed in 293T cells with a luciferase reporter (pFR-Luc) and GAL4-vIRF1, together with either VP16-GRIM19 or VP16. As shown in Fig. 2B, VP16-GRIM19 activated luciferase transcription via GAL4-vIRF1 in a dose-dependent manner, whereas VP16 did not. GAL4-vIRF1 expression was monitored by a Western blot assay, which revealed that levels of the chimeric protein re-

mained unchanged in the presence of both VP16-GRIM19 and VP16. These data indicate that vIRF1 physically interacts with GRIM19 in mammalian cells.

We next determined whether vIRF1 binds GRIM19 in vivo. 293T cells were cotransfected with GST, GST-GRIM19, and FLAG-vIRF1 expression plasmids (pEBG, pEBG-GRIM19, and pFIN-vIRF1, respectively). At 48 h after transfection, cells were lysed and incubated with glutathione-Sepharose 4B beads for 2 h to precipitate GST and GST-GRIM19 proteins. Precipitated proteins were immunoblotted with an anti-FLAG antibody. The FLAG-vIRF1 protein coprecipitated with GST-GRIM19 but not with GST alone (Fig. 3A, top panel). To establish that the FLAG-vIRF1, GST, and GST-GRIM19 proteins are expressed properly in transfected cells, we performed a Western blot assay by using total cell extracts with anti-FLAG and anti-GST antibodies (Fig. 3A, top and bottom panels, respectively). In a reciprocal experiment, 293T cells were cotransfected with FLAG-vIRF1 (pFIN-vIRF1) and HA-GRIM19 (pcDNA3-HA-GRIM19), lysed, and immunoprecipitated with an anti-FLAG antibody. The precipitated complex was immunoblotted with anti-HA antibody. HA-GRIM19 coimmunoprecipitated with FLAG-vIRF1, but not FLAG alone (Fig. 3B, top panel). HA-GRIM19 and FLAG-vIRF1 proteins were properly expressed from total cell extracts (Fig. 3B, top and bottom panels, respectively). To confirm the interactions between vIRF1 and GRIM19, we performed coimmunoprecipitation assays in KSHV-infected BCBL-1 cells. Since vIRF1 is a lytic protein, vIRF1 expression was induced with TPA (36) (Fig. 3C, left panel). Total lysates of BJAB and BCBL-1 cells were immunoblotted with anti-vIRF1 polyclonal antibody and anti-GRIM19 monoclonal antibody (Fig. 3C, right panel, lanes 1 and 2). Cells were lysed and immunoprecipitated with either anti-GRIM19 or anti-HA antibody. The vIRF1 protein coimmunoprecipitated with GRIM19 in KSHV-infected BCBL-1 cells (Fig. 3C, right panel, lane 4). However, vIRF1 was not detected in KSHV-negative BJAB cell extracts or by immunoprecipitation with anti-HA antibody (Fig. 3C, right panel, lanes 3 and 5). Our data confirm that vIRF1 interacts with GRIM19 in lymphocytes.

Since vIRF1 binds to CBP/p300 (4, 23, 40), it is possible that vIRF1-GRIM19 interaction is originated from bridging through CBP/p300. To exclude this bridge effect, we examined the in vivo interaction between GRIM19 and CBP. 293T cells were cotransfected with GST, GST-GRIM19, GST-vIRF1, and HA-CBP expression plasmids, lysed, and precipitated with glutathione-Sepharose 4B beads. The precipitated complex was immunoblotted with anti-HA monoclonal antibody. The GST-vIRF1 coprecipitated with CBP but not GST-GRIM19 (Fig. 3D, top panel). These data show that GRIM19 dose not interact with CBP, and therefore vIRF1-GRIM19 interaction is not caused by bridging CBP.

Colocalization of vIRF1 and GRIM19. To determine whether vIRF1 and GRIM19 complexes colocalize, we examined their subcellular localization by immunofluorescence confocal microscopy. 293T cells were transfected with GFP-GRIM19 (pEGFPC1-GRIM19) and FLAG-vIRF1 (pFIN-vIRF1) expression plasmids. As shown previously, GFP-GRIM19 was located within the nucleus, whereas GFP alone displayed a diffuse pattern throughout the cytoplasm and nucleus (1). The vIRF1 protein was observed throughout the cytoplasm and nucleus, although the large proportion was localized in the nucleus (Fig. 4A). In 293T cells coexpressing FLAG-vIRF1 and GFP-GRIM19, vIRF1 was colocalized with GFP-GRIM19 in the nucleus (Fig. 4B). To examine the colocalization of vIRF1 and GRIM19 in physiological conditions, we performed confocal microscopy in KSHV-infected BCBL-1 cells. TPA-induced BCBL-1 cells were fixed and incubated with anti-vIRF1 and anti-GRIM19 antibodies. vIRF1 also was colocalized with GRIM19 in the nucleus of BCBL-1 cells (Fig. 4C). This colocalization of vIRF1 and GRIM19 indicates specific interactions between the two proteins in vivo.

To confirm the exact subcellular localization of these two proteins, fractionated extracts from transfected cells were separated into nuclear and cytoplasmic fractions, and each fraction was analyzed by Western blotting (Fig. 4D). FLAG-vIRF1 was detected mainly in nuclear fraction and a small portion of FLAG-vIRF1 was detected in cytoplasmic fraction (Fig. 4D, top panel). GFP was detected in both nuclear and cytoplasmic fractions, but GFP-GRIM19 was detected only in nuclear fraction (Fig. 4D, bottom panel). The nuclear fractions from the cells expressing GFP, GFP-GRIM19, and FLAG-vIRF1 were immunoprecipitated with anti-GFP polyclonal antibody and immunoblotted with anti-FLAG monoclonal antibody. Nuclear FLAG-vIRF1 was coimmunoprecipitated with nuclear GFP-GRIM19 (Fig. 4E). These data indicate that vIRF1 associates GRIM19 in nucleus.

The N-terminal region of vIRF1 is required for interactions with GRIM19. To identify the region of vIRF1 that specifically binds GRIM19, we performed a GST pull-down assay. A series of GST-vIRF1 N-terminal and C-terminal deletion mutants were constructed, specifically, GST-vIRF1ΔC (aa 1 to 360), GST-vIRF1ΔC1 (aa 1 to 270), GST-vIRF1ΔC2 (aa 1 to 230), GST-vIRF1N (aa 1 to 152), GST-vIRF1ΔN (aa 152 to 449), and vIRF1C (aa 289 to 449) (Fig. 5A). In vitro-translated GRIM19 interacted with GST-vIRF1, GST-vIRF1ΔC, GST-vIRF1ΔC1, GST-vIRF1ΔC2, and GST-vIRF1N proteins, but not with GST-vIRF1ΔN and GST-vIRF1C (Fig. 5B). From these data, we conclude that the N-terminal region of vIRF1 is necessary for binding GRIM19.

vIRF1 deregulates GRIM19-induced apoptosis in response to IFN/RA. Since GRIM19 induces apoptotic cell death in response to the IFN/RA signal (1), we investigated whether vIRF1 regulates this activity. GRIM19 induced apoptosis that was strongly enhanced upon IFN/RA treatment, suggesting that the protein undergoes posttranslational modifications or interacts with other factors in the presence of IFN/RA (1). Consequently, we investigated cell apoptosis induced by GRIM19 in the presence of IFN/RA in this study. To examine the effects of vIRF1 on GRIM19-induced apoptosis by IFN/RA, a TUNEL assay was performed (15) in HeLa cells. Transiently transfected HeLa cells were treated with a IFN/RA combination for 72 h, fixed, and subjected to TUNEL analysis. Since the TUNEL reaction used FITC as a labeling reagent, TUNEL-positive (apoptotic) cells contained green nuclei. Transfection of the GRIM19 expression plasmid increased the number of TUNEL-positive cells in the presence of IFN/RA, whereas cotransfection of vIRF1 (pFIN-vIRF1) and GRIM19 expression plasmid (pCXN2-GRIM19) decreased the number of TUNEL-positive cells. However, cotransfection with vIRF1ΔN (pFIN-vIRF1ΔN) did not alter apoptosis by

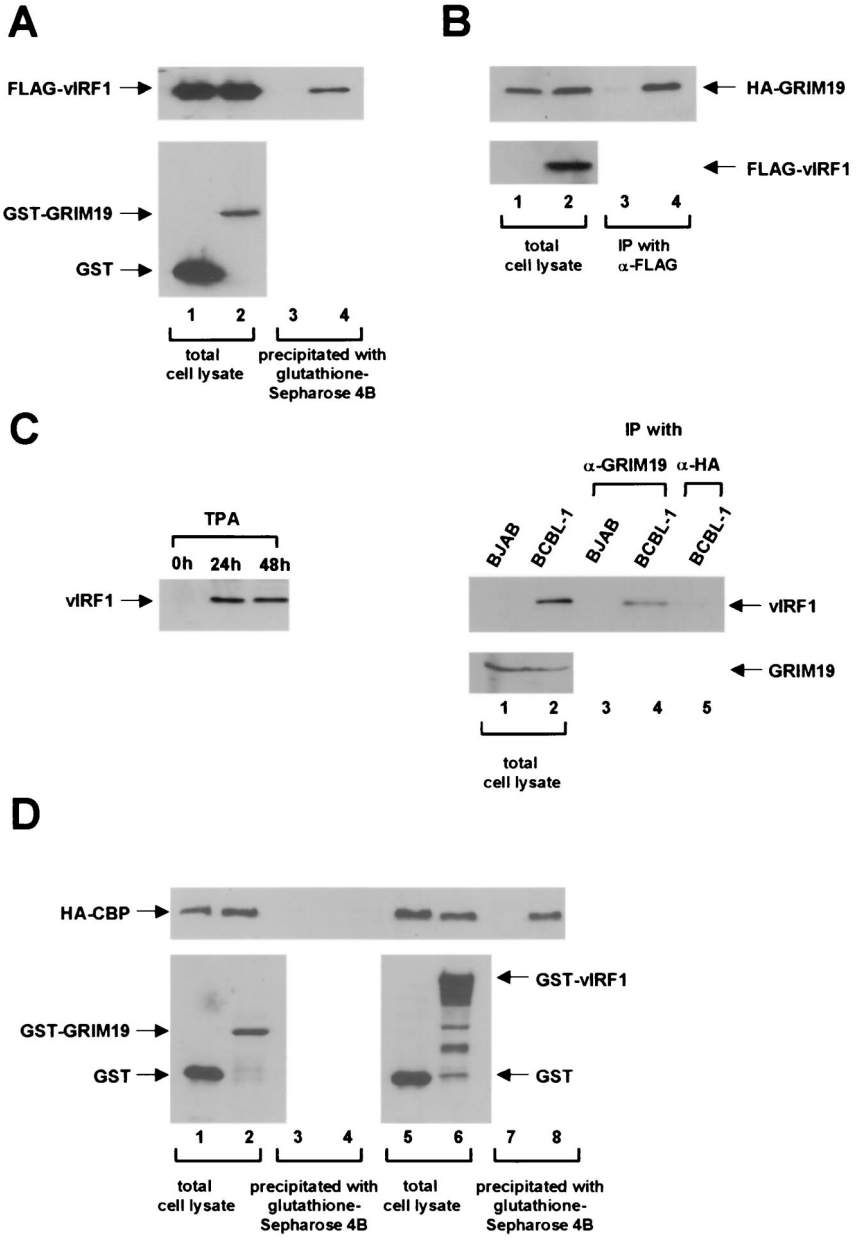

FIG. 3. Association of vIRF1 and GRIM19 in vivo. (A) A GST expression plasmid (pEBG) or a GST-GRIM19 expression plasmid (pEBG-GRIM19) was cotransfected with FLAG-vIRF1 expression plasmid (pFIN-vIRF1) into 293T cells. Cell extracts were precipitated with glutathione-Sepharose 4B. The resulting precipitates were washed and resolved by SDS-PAGE. GST fusion protein and FLAG-vIRF1 were detected by Western blotting with anti-FLAG (top panel) and anti-GST (bottom panel) antibodies, respectively. Lanes: 1 and 3, GST with FLAG-vIRF1; 2 and 4, GST-GRIM19 with FLAG-vIRF1. (B) An HA-GRIM19 expression plasmid (pcDNA3-HA-GRIM19) was cotransfected with or without the FLAG-vIRF1 expression plasmid (pFIN-vIRF1). Cell extracts were immunoprecipitated with anti-FLAG monoclonal antibody, washed, and resolved by SDS-PAGE. HA-GRIM19 and FLAG-vIRF1 were detected by Western blotting with anti-HA (top panel) and anti-FLAG (bottom panel). Lanes: 1 and 3, HA-GRIM19 alone; 2 and 4, HA-GRIM19 with FLAG-vIRF1. IP, immunoprecipitation. (C) vIRF1 associates with GRIM19 in KSHV-infected BCBL-1 cells. BCBL-1 cells were treated with TPA as previously described (36) and cell extracts were prepared after the indicated number of hours. vIRF1 was detected by Western blotting with anti-vIRF1 polyclonal antibody (left panel). A coimmunoprecipitation assay was performed with BJAB and BCBL-1 cells (2×10^7 cells) after 48 h of TPA induction. Total cell extracts were immunoblotted with anti-vIRF1 and anti-GRIM19, respectively (lanes 1 and 2). Cell extracts were immunoprecipitated with anti-GRIM19 monoclonal antibody (lanes 3 and 4) and anti-HA monoclonal antibody (lane 5). vIRF1 was detected by Western blotting with anti-vIRF1 polyclonal antibody (right top panel). (D) GRIM19 does not interact with CBP. A GST expression plasmid (pEBG), a GST-GRIM19 expression plasmid (pEBG-GRIM19), or a GST-vIRF1 expression plasmid (pEBG-vIRF1) was cotransfected with HA-CBP expression plasmid (pCMV-HA-CBP) into 293T cells. Cell extracts were precipitated with glutathione-Sepharose 4B. The resulting precipitates were washed and resolved by SDS-PAGE. GST fusion proteins and HA-CBP were detected by Western blotting with anti-HA (top panel) and anti-GST (bottom panel) antibodies. Lanes: 1 and 3, GST with HA-CBP; 2 and 4, GST-GRIM19 with HA-CBP; 5 and 7, GST with HA-CBP; 6 and 8, GST-vIRF1 with HA-CBP.

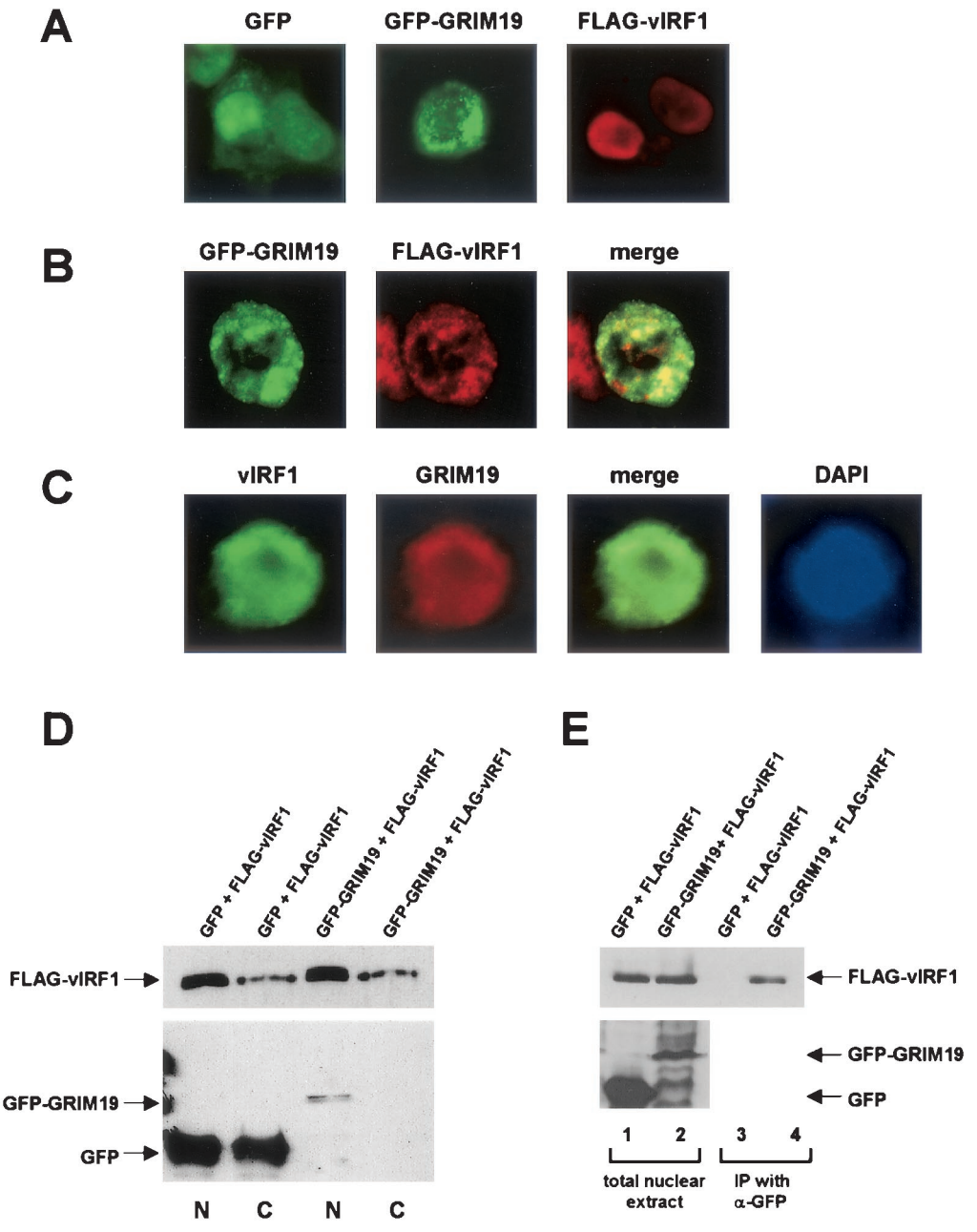

FIG. 4. Colocalization of vIRF1 and GRIM19. Immunofluorescence analyses were performed by using a Zeiss confocal microscope. (A) 293T cells were transfected with expression plasmids containing GFP, GFP-GRIM19, and FLAG-vIRF1. Cells expressing FLAG-vIRF1 were fixed after 48 h of transfection, incubated with anti-FLAG antibody, and detected with TRITC-conjugated anti-mouse antibody. (B) Colocalization of vIRF1 and GRIM19 in 293T cells. The yellow color in the merged panel indicates the colocalization of green and red colors. (C) Colocalization of vIRF1 and GRIM19 in KSHV-infected BCBL-1 cells. After 48 h of TPA induction, BCBL-1 cells were fixed and incubated with anti-vIRF1 polyclonal and anti-GRIM19 monoclonal antibodies. vIRF1 was detected with FITC-conjugated anti-rabbit antibody, and GRIM19 was detected with TRITC-conjugated anti-mouse antibody. The nucleus of the cell was stained with DAPI. (D) Nuclear and cytoplasmic extracts from 293T cells transfected with FLAG-vIRF1 expression plasmid (pFIN-vIRF1) and either GFP expression plasmid (pEGFP-C1) or GFP-GRIM19 expression plasmid (pEGFP-C1-GRIM19) were analyzed by Western blotting. N, nuclear fraction; C, cytoplasmic fraction. (E) vIRF1 interacts with GRIM19 in the nucleus. Nuclear fractions from 293T cells expressing FLAG-vIRF1 in combination with either GFP or GFP-GRIM19 were immunoprecipitated with anti-GFP polyclonal anitibody, washed, and resolved by SDS-PAGE. FLAG-vIRF1, GFP, and GFP-GRIM19 were analyzed by Western blotting. Lanes: 1 and 3, GFP with FLAG-vIRF1; 2 and 4, GFP-GRIM19 with FLAG-vIRF1.

GRIM19 (Fig. 6A). The vIRF1ΔN protein did not interact with GRIM19 in a GST pull-down assay (Fig. 5B). Therefore, protein-protein interactions between vIRF1 and GRIM19 are required for the inhibition of GRIM19-mediated apoptosis. Apoptotic cells in the presence of IFN/RA represented 19.1, 58.7, 16.8, 54.1, and 8.9% of the total cell population during expression of no protein, GRIM19, GRIM19 in combination with vIRF1, GRIM19 plus vIRF1ΔN, and vIRF1, respectively (Fig.

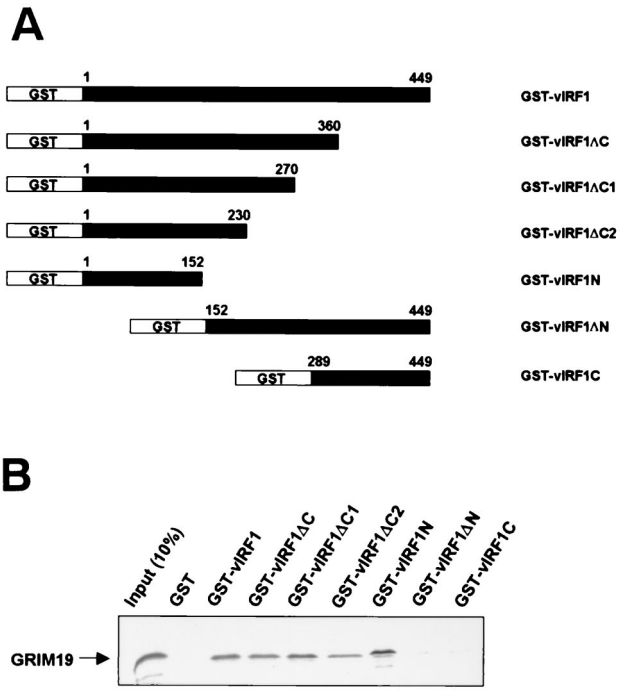

FIG. 5. Mapping of the vIRF1 domain required for binding to GRIM19. (A) Schematic representation of GST-vIRF1 and its mutants employed in a GST pull-down assay. (B) The GST pull-down assay was performed with GST-vIRF1 and its deletion mutants by using ^{35}S-labeled in vitro-translated GRIM19. The input (10%) and GST pull-down mixtures were resolved by SDS-PAGE and visualized by autoradiography.

6B). These results suggest that vIRF1 inhibits the apoptotic activity of GRIM19.

vIRF1 suppresses IFN/RA-induced cell death. Since GRIM19 plays a critical role in IFN/RA cell death (1), we investigated whether vIRF1 deregulates this process. MCF-7 cells were stably transfected with vector (pFIN), FLAG-vIRF1 (pFIN-vIRF1), and the N-terminal 151-aa deletion mutant (pFIN-vIRF1ΔN) that does not interact with GRIM19 (Fig. 5B). Successfully transfected cells were selected in medium containing G418 (1 mg/ml) for 3 weeks. To determine whether cells expressing vIRF1 are resistant to the apoptotic effect of IFN/RA compared to those expressing vector alone, we monitored the growth of MCF-7 stable cells in the presence of IFN/RA by using the SRB assay (42). Cell growth was measured after 3, 5, and 7 days and is presented as a percentage of IFN/RA-untreated cells. The results demonstrate that MCF-7 cells expressing vIRF1 are more resistant to IFN/RA-induced cell death than those expressing vIRF1ΔN or vector alone (Fig. 7A). vIRF1ΔN does not associate with GRIM19 (Fig. 5B), indicating that binding between these two proteins is important for inhibiting IFN/RA-induced cell death. Expression of vIRF1 and vIRF1ΔN was detected by Western blotting with anti-FLAG (Fig. 7B) antibody. The data suggest that vIRF1 inhibits the cell death-promoting activity of IFN/RA.

Human papillomavirus type 16 (HPV-16) E6 interacts with GRIM19. To investigate the possibility that DNA tumor virus proteins other than KSHV vIRF1 also target GRIM19, we examined the interaction between HPV-16 E6 and GRIM19. 293T cells were cotransfected with GST, GST-GRIM19, and FLAG-16 E6 expression plasmids (pEBG, pEBG-GRIM19, and pME18S-16 E6, respectively). At 48 h after transfection, cells were lysed and incubated with glutathione-Sepharose 4B beads for 2 h to precipitate GST and GST-GRIM19 proteins. Precipitated proteins were immunoblotted with an anti-FLAG antibody. The FLAG-16 E6 protein coprecipitated with GST-GRIM19 but not with GST alone (Fig. 8A, top panel). These data show that HPV-16 E6 interacts with GRIM19 in vivo.

HPV E6 proteins of the low-risk group associate with p53 with lower affinity than HPV E6 proteins of the high-risk group (46). To determine whether GRIM19 binding also differs between the high- and low-risk groups of HPV E6, we performed GST pull-down assays with in vitro-translated HPV-11 E6 (low risk) and HPV-16 E6 (high risk). GST-GRIM19 was immobilized on glutathione-Sepharose 4B beads, and binding of in vitro-translated 11 E6, 16 E6, and luciferase to the fusion protein was observed. Luciferase (used as a negative control) did not interact with GST-GRIM19. HPV-16 E6 specifically associated with GRIM19 more strongly than HPV-11 E6, suggesting that the difference between high-risk and low-risk E6-GRIM19 interaction correlates with the transforming activity of these different papillomaviruses (Fig. 8B). Interestingly, both vIRF1 and HPV-16 E6 interact with p53, p300/CBP, and GRIM19, suggesting that the two proteins share cellular interaction partners. We also examined the interaction of SV40 LT antigen and adenovirus E1A to GRIM19. In GST pull-down assays, SV40 LT antigen also interacted with GRIM19, but E1A did not (data not shown). The finding that DNA tumor viral proteins other than vIRF1 interact with GRIM19 suggests that GRIM19 may be a general target for tumor viral proteins.

DISCUSSION

Sequence analyses reveal that KSHV ORFs encode a number of accessory proteins that display significant homology to cellular regulatory proteins and an unusual degree of genetic piracy compared to other herpesviruses (13, 32, 39). Many of these viral genes encode proteins that deregulate cellular gene expression or signaling, including vCyclin (ORF72), vBCL-2 (ORF16), vGPCR (ORF74), vIRF1 (ORFK9), vIL-6 (ORFK2), and vFLIP (ORFK13) (32). Among these, vIRF1 triggers the transformation of NIH 3T3 cells, leading to malignant tumors in nude mice (14, 24). The vIRF1 protein effectively blocks IFN- and IRF1-mediated transcription. However, the issue of whether vIRF1 and IRF1 directly interact is currently controversial (4, 48). Since IRF1 is a tumor suppressor, it is hypothesized that the tumor-inducing activity of vIRF1 is partly caused by inhibition of IRF1 (48). vIRF1 additionally influences cellular regulation pathways other than the IFN pathway. Previous studies established that vIRF1 interacts with p300/CBP and inhibits the histone acetyltransferase activity of p300 (4, 23, 40). In addition, vIRF1 associates with p53, resulting in the inhibition of p53-dependent apoptosis (33, 41). These data specify the various functions of vIRF1 and partly explain the molecular mechanism of vIRF1-transforming activity. In this report, we demonstrate that GRIM19 is a cellular interaction partner of vIRF1. Moreover, vIRF1 inhibits GRIM19-induced apoptosis in HeLa cells and suppresses IFN/RA-mediated death in MCF-7 cells. Direct inter-

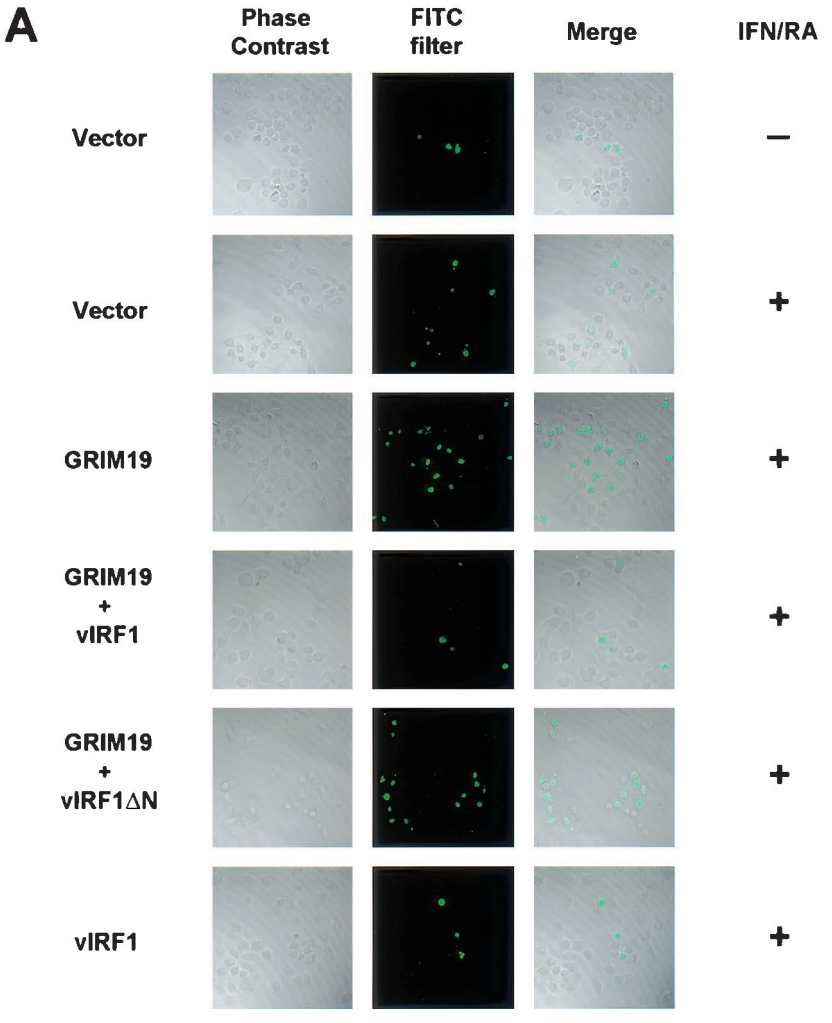

FIG. 6. vIRF1 deregulates GRIM19-induced apoptosis in the presence of IFN/RA. HeLa cells grown on a coverslip in 35-mm-diameter dishes were transfected with GRIM19 expression plasmid (pCXN2-GRIM19), N-terminal deletion vIRF1 expression plasmid (pFIN-vIRF1ΔN), and vIRF1 expression plasmid (pFIN-vIRF1) by using the Superfect transfection reagent. Cells were treated with IFN-β (3,000 U/ml) in combination with RA (5 μM) for 72 h and fixed, after which the TUNEL reaction was performed. Analyses were performed by using a Zeiss confocal microscope. (A) The left panel displays phase-contrast images of cells observed under a bright field. The center panel shows the images of TUNEL-positive cells under FITC filter sets. The right panel displays the merged images. (B) TUNEL-positive apoptotic cells are represented as a percentage of apoptosis. The bar specifies the percentage of transfected cells undergoing apoptosis, as determined by counting the dead cells stained green. Each bar represents the mean of two duplicate samples. At least 500 cells were counted from various fields.

actions between vIRF1 and GRIM19 are required for these activities.

GRIM19 is a newly characterized death-regulatory protein whose inactivation leads to growth advantage to cells in the presence of IFN/RA. However, mechanism of IFN/RA-mediated cell death is yet to be fully elucidated. GRIM19 is located at the 19p13.2 locus of the human chromosome essential for prostate tumor progression. This supports the possibility that the protein acts as a tumor suppressor. Interestingly, Fearnley et al. (11) reported that bovine GRIM19 is a subunit of bovine mitochondrial complex I, a finding suggesting the involvement of mitochondria in GRIM19-induced apoptotic cell death. These results collectively indicate that GRIM19 plays a critical role in cell death, although the biochemical function of

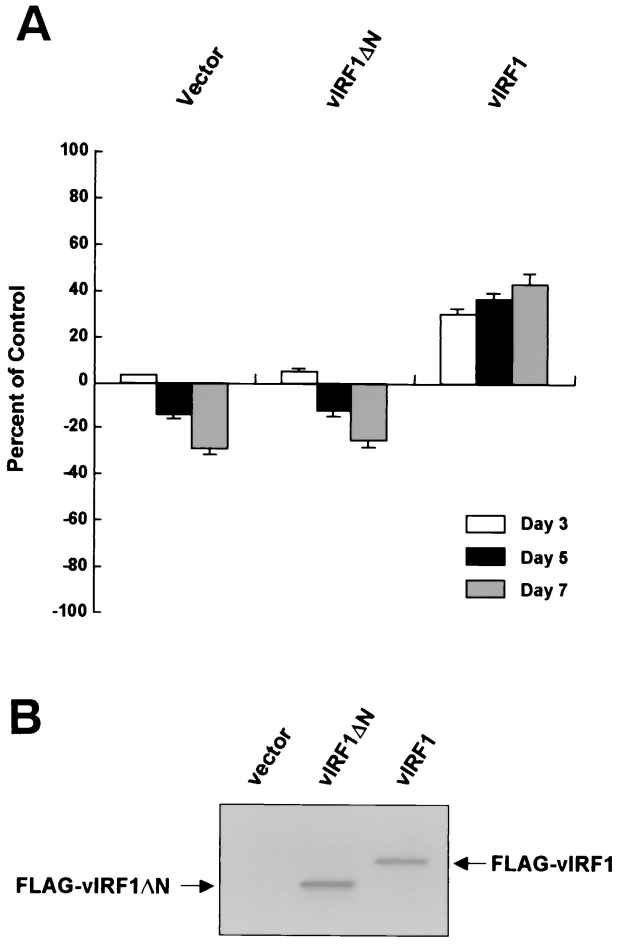

FIG. 7. vIRF1 inhibits IFN/RA-induced cell death. (A) The growth of MCF-7 cells stably expressing vector, FLAG-vIRF1ΔN, and FLAG-vIRF1 was monitored by the SRB method (42) as described in Materials and Methods. Cells were treated with IFN-β (500 U/ml) in combination with RA (1 μM). The absorbance value at 570 nm for 0% growth is 0.252, 0.284, and 0.291, respectively. The 100% growth absorbance values for 3, 5, and 7 days are: 0.632, 0.605, and 0.836; 0.974, 0.938, and 1.272; 1.332, 1.259, and 1.673; and 1.810, 1.580, and 2.186. Each value represents a mean of eight replicates. (B) Total cell extracts were prepared from MCF-7 cells expressing vector, FLAG-vIRF1ΔN, and FLAG-vIRF1. Extracts were resolved by SDS-PAGE and immunoblotted with anti-FLAG monoclonal antibody.

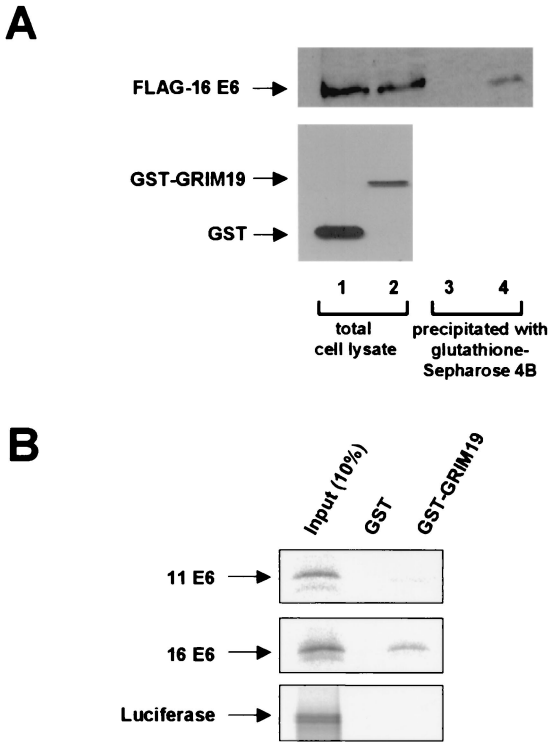

FIG. 8. GRIM19 interacts with HPV-16 E6. (A) A GST expression plasmid (pEBG) or a GST-GRIM19 expression plasmid (pEBG-GRIM19) was cotransfected with FLAG-16 E6 expression plasmid (pME18S-16 E6) into 293T cells. Cell extracts were precipitated with glutathione-Sepharose 4B. The resulting precipitates were washed and resolved by SDS-PAGE. GST fusion protein and FLAG-16 E6 were detected by Western blotting with anti-FLAG (top panel) and anti-GST (bottom panel) antibodies. Lanes: 1 and 3, GST with FLAG-16 E6; 2 and 4, GST-GRIM19 with FLAG-16 E6. (B) GST pull-down assays were performed with GST-GRIM19, ^{35}S-labeled HPV-11 E6, HPV-16 E6, and luciferase. Each input (10%) and GST pull-down mixture was resolved by SDS-PAGE and visualized by autoradiography.

GRIM19 is unclear. Angell et al. (1) showed that the C-terminal region of GRIM19 harboring a putative ATP-binding domain, IMKDVPXWKVGE, is required for cell death induction. This region is highly conserved throughout various eukaryotic GRIM19 homologs. One possible mechanism of GRIM19 inhibition involves targeting the ATP-binding domain by vIRF1, which would result in the abrogation of apoptotic activity. Although we demonstrate the importance of vIRF1 and GRIM19 binding in suppressing IFN/RA-induced cell death, we cannot exclude the possibility of interactions between vIRF1 and other GRIMs or other cellular factors that may play an important role in IFN/RA signaling.

NIH 3T3 cells expressing vIRF1 are resistant to tumor necrosis factor alpha-induced apoptosis, although the mechanism for this is currently unknown (4). Human B lymphocytes expressing vIRF1 are resistant to the antiproliferative effects of IFN-α, and vIRF1 expression inhibits p53-induced apoptosis (12, 33, 41). MCF-7 cells expressing vIRF1 are also resistant to IFN/RA-induced cell death, possibly through interactions between vIRF1 and GRIM19 (Fig. 7). These data strongly suggest that vIRF1 induces resistance in cells to various death signals. Cells expressing vIRF1 may be resistant to other cell death signals, such as those of Fas ligand and hypoxia. Further studies are required to confirm whether vIRF1 inhibits cell death induced by other factors. The resistance to a number of cell death and antiproliferative signals is consistent with the strong transforming activity of vIRF1.

The vIRF1 interaction partners, p300/CBP and p53, are commonly targeted by other DNA viral oncoproteins, such as SV40 LT antigen, HPV E6 and adenovirus E1A (2, 10, 21, 34, 46). In view of this observation, we hypothesize that if GRIM19 acts as tumor suppressor in multiple tissues, it may be a general target for tumor viral proteins other than vIRF1. In vitro and in vivo binding assays reveal that HPV-16 E6 specifically interacts with GRIM19 (Fig. 8). Interestingly, GRIM19 binds more strongly to high-risk group E6 than to low-risk

group E6, suggesting the possibility that E6-GRIM19 interaction may contribute to the transforming activity of high-risk group E6. We are currently investigating whether E6 also deregulates IFN/RA-mediated cell death. During viral oncogenesis, GRIM19 may be a general target protein similar to other cellular tumor suppressors, such as p53, p300/CBP, and RB. Further studies are required to elucidate the importance of GRIM19 protein in oncogenesis of the DNA tumor virus.

ACKNOWLEDGMENTS

This work was supported in part by grants from the National Research Laboratory Program of the Korea Institute of Science and Technology Evaluation and Planning (KISTEP), the Korea Science and Engineering Foundation (KOSEF) through the Protein Network Research Center at Yonsei University, and the BK21 Program of the Ministry of Education Korea. D.V.K. was supported by grant CA78282 from the National Cancer Institute, National Institutes of Health.

REFERENCES

1. **Angell, J. E., D. J. Lindner, P. S. Shapiro, E. R. Hofmann, and D. V. Kalvakolanu.** 2000. Identification of GRIM-19, a novel cell death-regulatory gene induced by the interferon-beta and retinoic acid combination, using a genetic approach. J. Biol. Chem. **275:**33416–33426.
2. **Arany, Z., D. Newsome, E. Oldread, D. M. Livingston, and R. Eckner.** 1995. A family of transcriptional adaptor proteins targeted by the E1A oncoprotein. Nature **374:**81–84.
3. **Burysek, L., and P. M. Pitha.** 2001. Latently expressed human herpesvirus 8-encoded interferon regulatory factor 2 inhibits double-stranded RNA-activated protein kinase. J. Virol. **75:**2345–2352.
4. **Burysek, L., W. S. Yeow, B. Lubyova, M. Kellum, S. L. Schafer, Y. Q. Huang, and P. M. Pitha.** 1999. Functional analysis of human herpesvirus 8-encoded viral interferon regulatory factor 1 and its association with cellular interferon regulatory factors and p300. J. Virol. **73:**7334–7342.
5. **Cesarman, E., Y. Chang, P. S. Moore, J. W. Said, and D. M. Knowles.** 1995. Kaposi's sarcoma-associated herpesvirus-like DNA sequences in AIDS-related body-cavity-based lymphomas. N. Engl. J. Med. **332:**1186–1191.
6. **Chang, Y., E. Cesarman, M. S. Pessin, F. Lee, J. Culpepper, D. M. Knowles, and P. S. Moore.** 1994. Identification of herpesvirus-like DNA sequences in AIDS-associated Kaposi's sarcoma. Science **266:**1865–1869.
7. **Chidambaram, N. V., J. E. Angell, W. Ling, E. R. Hofmann, and D. V. Kalvakolanu.** 2000. Chromosomal localization of human GRIM-19, a novel IFN-beta and retinoic acid-activated regulator of cell death. J. Interferon Cytokine Res. **20:**661–665.
8. **Deiss, L. P., and A. Kimchi.** 1991. A genetic tool used to identify thioredoxin as a mediator of a growth inhibitory signal. Science **252:**117–120.
9. **Durfee, T., K. Becherer, P. L. Chen, S. H. Yeh, Y. Yang, A. E. Kilburn, W. H. Lee, and S. J. Elledge.** 1993. The retinoblastoma protein associates with the protein phosphatase type 1 catalytic subunit. Genes Dev. **7:**555–569.
10. **Eckner, R., J. W. Ludlow, N. L. Lill, E. Oldread, Z. Arany, N. Modjtahedi, J. A. DeCaprio, D. M. Livingston, and J. A. Morgan.** 1996. Association of p300 and CBP with simian virus 40 large T antigen. Mol. Cell. Biol. **16:**3454–3464.
11. **Fearnley, I. M., J. Carroll, R. J. Shannon, M. J. Runswick, J. E. Walker, and J. Hirst.** 2001. Grim-19, a cell death regulatory gene product, is a subunit of bovine mitochondrial nadh:ubiquinone oxidoreductase (complex i). J. Biol. Chem. **276:**38345–38348.
12. **Flowers, C. C., S. P. Flowers, and G. J. Nabel.** 1998. Kaposi's sarcoma-associated herpesvirus viral interferon regulatory factor confers resistance to the antiproliferative effect of interferon-alpha. Mol. Med. **4:**402–412.
13. **Ganem, D.** 1997. KSHV and Kaposi's sarcoma: the end of the beginning? Cell **91:**157–160.
14. **Gao, S. J., C. Boshoff, S. Jayachandra, R. A. Weiss, Y. Chang, and P. S. Moore.** 1997. KSHV ORF K9 (vIRF) is an oncogene which inhibits the interferon signaling pathway. Oncogene **15:**1979–1985.
15. **Gorczyca, W., K. Bigman, A. Mittelman, T. Ahmed, J. Gong, M. R. Melamed, and Z. Darzynkiewicz.** 1993. Induction of DNA strand breaks associated with apoptosis during treatment of leukemias. Leukemia **7:**659–670.
16. **Graham, F. L., and A. J. van der Eb.** 1973. A new technique for the assay of infectivity of human adenovirus 5 DNA. Virology **52:**456–467.
17. **Harada, H., M. Kitagawa, N. Tanaka, H. Yamamoto, K. Harada, M. Ishihara, and T. Taniguchi.** 1993. Anti-oncogenic and oncogenic potentials of interferon regulatory factors-1 and -2. Science **259:**971–974.
18. **Hofmann, E. R., M. Boyanapalli, D. J. Lindner, X. Weihua, B. A. Hassel, R. Jagus, P. L. Gutierrez, D. V. Kalvakolanu, and E. R. Hofman.** 1998. Thioredoxin reductase mediates cell death effects of the combination of beta interferon and retinoic acid. Mol. Cell. Biol. **18:**6493–6504.
19. **James, P., J. Halladay, and E. A. Craig.** 1996. Genomic libraries and a host strain designed for highly efficient two-hybrid selection in yeast. Genetics **144:**1425–1436.
20. **Kumar, A., M. Commane, T. W. Flickinger, C. M. Horvath, and G. R. Stark.** 1997. Defective TNF-α-induced apoptosis in STAT1-null cells due to low constitutive levels of caspases. Science **278:**1630–1632.
21. **Lane, D. P., and L. V. Crawford.** 1979. T antigen is bound to a host protein in SV40-transformed cells. Nature **278:**261–263.
22. **Lee, D., B. Lee, J. Kim, D. W. Kim, and J. Choe.** 2000. cAMP response element-binding protein-binding protein binds to human papillomavirus E2 protein and activates E2-dependent transcription. J. Biol. Chem. **275:**7045–7051.
23. **Li, M., B. Damania, X. Alvarez, V. Ogryzko, K. Ozato, and J. U. Jung.** 2000. Inhibition of p300 histone acetyltransferase by viral interferon regulatory factor. Mol. Cell. Biol. **20:**8254–8263.
24. **Li, M., H. Lee, J. Guo, F. Neipel, B. Fleckenstein, K. Ozato, and J. U. Jung.** 1998. Kaposi's sarcoma-associated herpesvirus viral interferon regulatory factor. J. Virol. **72:**5433–5440.
25. **Lin, R., P. Genin, Y. Mamane, M. Sgarbanti, A. Battistini, W. J. Harrington, Jr., G. N. Barber, and J. Hiscott.** 2001. HHV-8 encoded vIRF-1 represses the interferon antiviral response by blocking IRF-3 recruitment of the CBP/p300 coactivators. Oncogene **20:**800–811.
26. **Lindner, D. J., E. C. Borden, and D. V. Kalvakolanu.** 1997. Synergistic antitumor effects of a combination of interferons and retinoic acid on human tumor cells in vitro and in vivo. Clin. Cancer Res. **3:**931–937.
27. **Lotan, R.** 1994. Suppression of squamous cell carcinoma growth and differentiation by retinoids. Cancer Res. **54:**1987–1990.
28. **Lotan, R., M. I. Dawson, C. C. Zou, L. Jong, D. Lotan, and C. P. Zou.** 1995. Enhanced efficacy of combinations of retinoic acid- and retinoid X receptor-selective retinoids and alpha-interferon in inhibition of cervical carcinoma cell proliferation. Cancer Res. **55:**232–236.
29. **Lubyova, B., and P. M. Pitha.** 2000. Characterization of a novel human herpesvirus 8-encoded protein, vIRF-3, that shows homology to viral and cellular interferon regulatory factors. J. Virol. **74:**8194–8201.
30. **Ma, X., S. Karra, W. Guo, D. J. Lindner, J. Hu, J. E. Angell, E. R. Hofmann, S. P. Reddy, and D. V. Kalvakolanu.** 2001. Regulation of interferon and retinoic acid-induced cell death activation through thioredoxin reductase. J. Biol. Chem. **276:**24843–24854.
31. **Moore, D. M., D. V. Kalvakolanu, S. M. Lippman, J. J. Kavanagh, W. K. Hong, E. C. Borden, M. Paredes-Espinoza, and I. H. Krakoff.** 1994. Retinoic acid and interferon in human cancer: mechanistic and clinical studies. Semin. Hematol. **31:**31–37.
32. **Moore, P. S., and Y. Chang.** 1998. Antiviral activity of tumor-suppressor pathways: clues from molecular piracy by KSHV. Trends Genet. **14:**144–150.
33. **Nakamura, H., M. Li, J. Zarycki, and J. U. Jung.** 2001. Inhibition of p53 tumor suppressor by viral interferon regulatory factor. J. Virol. **75:**7572–7582.
34. **Patel, D., S. M. Huang, L. A. Baglia, and D. J. McCance.** 1999. The E6 protein of human papillomavirus type 16 binds to and inhibits co-activation by CBP and p300. EMBO J. **18:**5061–5072.
35. **Ploegh, H. L.** 1998. Viral strategies of immune evasion. Science **280:**248–253.
36. **Renne, R., W. Zhong, B. Herndier, M. McGrath, N. Abbey, D. Kedes, and D. Ganem.** 1996. Lytic growth of Kaposi's sarcoma-associated herpesvirus (human herpesvirus 8) in culture. Nat. Med. **2:**342–346.
37. **Rivas, C., A. E. Thlick, C. Parravicini, P. S. Moore, and Y. Chang.** 2001. Kaposi's sarcoma-associated herpesvirus LANA2 is a B-cell-specific latent viral protein that inhibits p53. J. Virol. **75:**429–438.
38. **Roan, F., J. C. Zimring, S. Goodbourn, and M. K. Offermann.** 1999. Transcriptional activation by the human herpesvirus-8-encoded interferon regulatory factor. J. Gen. Virol. **80:**2205–2209.
39. **Russo, J. J., R. A. Bohenzky, M. C. Chien, J. Chen, M. Yan, D. Maddalena, J. P. Parry, D. Peruzzi, I. S. Edelman, Y. Chang, and P. S. Moore.** 1996. Nucleotide sequence of the Kaposi sarcoma-associated herpesvirus (HHV8). Proc. Natl. Acad. Sci. USA **93:**14862–14867.
40. **Seo, T., D. Lee, B. Lee, J. H. Chung, and J. Choe.** 2000. Viral interferon regulatory factor 1 of Kaposi's sarcoma-associated herpesvirus (human herpesvirus 8) binds to, and inhibits transactivation of, CREB-binding protein. Biochem. Biophys. Res. Commun. **270:**23–27.
41. **Seo, T., J. Park, D. Lee, S. G. Hwang, and J. Choe.** 2001. Viral interferon regulatory factor 1 of Kaposi's sarcoma-associated herpesvirus binds to p53 and represses p53-dependent transcription and apoptosis. J. Virol. **75:**6193–6198.
42. **Skehan, P., R. Storeng, D. Scudiero, A. Monks, J. McMahon, D. Vistica, J. T. Warren, H. Bokesch, S. Kenney, and M. R. Boyd.** 1990. New colorimetric cytotoxicity assay for anticancer-drug screening. J. Natl. Cancer Inst. **82:**1107–1112.
43. **Soulier, J., L. Grollet, E. Oksenhendler, P. Cacoub, D. Cazals-Hatem, P. Babinet, M. F. d'Agay, J. P. Clauvel, M. Raphael, L. Degos, and F. Sigaux.** 1995. Kaposi's sarcoma-associated herpesvirus-like DNA sequences in multicentric Castleman's disease. Blood **86:**1276–1280.

44. **Tanaka, N., M. Ishihara, M. Kitagawa, H. Harada, T. Kimura, T. Matsuyama, M. S. Lamphier, S. Aizawa, T. W. Mak, and T. Taniguchi.** 1994. Cellular commitment to oncogene-induced transformation or apoptosis is dependent on the transcription factor IRF-1. Cell **77:**829–839.
45. **Warrell, R. P., Jr., H. de The, Z. Y. Wang, and L. Degos.** 1993. Acute promyelocytic leukemia. N. Engl. J. Med. **329:**177–189.
46. **Werness, B. A., A. J. Levine, and P. M. Howley.** 1990. Association of human papillomavirus types 16 and 18 E6 proteins with p53. Science **248:**76–79.
47. **Ye, Q., and H. J. Worman.** 1995. Protein-protein interactions between human nuclear lamins expressed in yeast. Exp. Cell Res. **219:**292–298.
48. **Zimring, J. C., S. Goodbourn, and M. K. Offermann.** 1998. Human herpesvirus 8 encodes an interferon regulatory factor (IRF) homolog that represses IRF-1-mediated transcription. J. Virol. **72:**701–707.